

Bulk GaN flip-chip violet light-emitting diodes with optimized efficiency for high-power operation

Christophe A. Humni, Aurelien David, Michael J. Cich, Rafael I. Aldaz, Bryan Ellis, Kevin Huang, Anurag Tyagi, Remi A. DeLille, Michael D. Craven, Frank M. Steranka, and Michael R. Krames

Citation: *Applied Physics Letters* **106**, 031101 (2015); doi: 10.1063/1.4905873

View online: <http://dx.doi.org/10.1063/1.4905873>

View Table of Contents: <http://scitation.aip.org/content/aip/journal/apl/106/3?ver=pdfcov>

Published by the [AIP Publishing](#)

Articles you may be interested in

[Analysis of micro-lens integrated flip-chip InGaN light-emitting diodes by confocal microscopy](#)

Appl. Phys. Lett. **104**, 051107 (2014); 10.1063/1.4863925

[Bulk GaN based violet light-emitting diodes with high efficiency at very high current density](#)

Appl. Phys. Lett. **101**, 223509 (2012); 10.1063/1.4769228

[Enhanced light extraction efficiency in flip-chip GaN light-emitting diodes with diffuse Ag reflector on nanotextured indium-tin oxide](#)

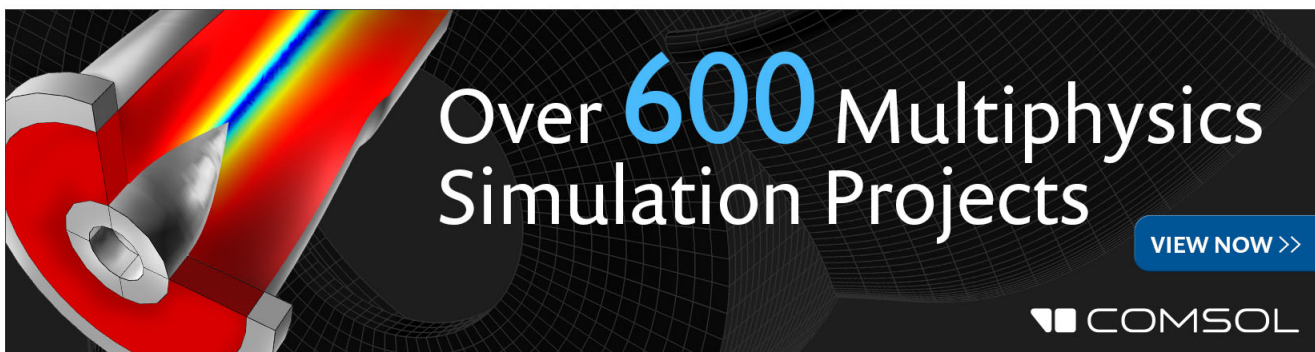
Appl. Phys. Lett. **93**, 021121 (2008); 10.1063/1.2953174

[Optical cavity effects in InGaN/GaN quantum-well-heterostructure flip-chip light-emitting diodes](#)

Appl. Phys. Lett. **82**, 2221 (2003); 10.1063/1.1566098

[High-power AlGaInN flip-chip light-emitting diodes](#)

Appl. Phys. Lett. **78**, 3379 (2001); 10.1063/1.1374499

The advertisement features a 3D simulation of a light-emitting diode (LED) structure. A red and yellow light beam is shown emanating from the device. The background is dark with a grid pattern. The text 'Over 600 Multiphysics Simulation Projects' is prominently displayed in white and blue. A blue button with the text 'VIEW NOW >>' is located in the bottom right corner. The COMSOL logo is also present in the bottom right corner.

Over **600** Multiphysics Simulation Projects

[VIEW NOW >>](#)

COMSOL

Bulk GaN flip-chip violet light-emitting diodes with optimized efficiency for high-power operation

Christophe A. Hurni,^{a)} Aurelien David, Michael J. Cich, Rafael I. Aldaz, Bryan Ellis, Kevin Huang, Anurag Tyagi, Remi A. DeLille, Michael D. Craven, Frank M. Steranka, and Michael R. Krames
 Soraa, Inc., 6500 Kaiser Dr., Fremont, California 94555, USA

(Received 25 November 2014; accepted 10 December 2014; published online 20 January 2015)

We report on violet-emitting III-nitride light-emitting diodes (LEDs) grown on bulk GaN substrates employing a flip-chip architecture. Device performance is optimized for operation at high current density and high temperature, by specific design consideration for the epitaxial layers, extraction efficiency, and electrical injection. The power conversion efficiency reaches a peak value of 84% at 85 °C and remains high at high current density, owing to low current-induced droop and low series resistance. © 2015 AIP Publishing LLC. [<http://dx.doi.org/10.1063/1.4905873>]

Thanks to dramatic progress since their invention in the early 1990s,¹ III-nitride based light-emitting diodes (LEDs) have been recognized as a practical solution for energy-efficient general lighting. Improved performance is still actively pursued as it enables further energy savings and reductions to overall product costs.² To date, the incumbent technology is based on hetero-epitaxy using substrates such as sapphire, silicon, or silicon carbide. In recent years, however, significant progress in the quality of quasi-bulk GaN substrates has enabled a radically different approach using homo-epitaxy, with advantages in all aspects of device performance from epitaxial quality to chip architecture.^{3–5} In Ref. 6, we discussed some of these advantages and presented data on violet LEDs grown on bulk GaN substrates with high external quantum efficiency at high current density.

In the present letter, we build upon this previous work and demonstrate how the various advantages of this technology can be systematically combined to obtain very high performance at high operating current and temperature. We introduce an improved architecture: triangular volumetric flip-chip⁷ LEDs, which leverages the benefits of bulk GaN substrates on many levels. We present a breakdown of device performance and demonstrate state-of-the-art results for each figure of merit.

We employ commercial low dislocation density quasi-bulk GaN substrates and grow epitaxial layers by metal-organic chemical vapor deposition. The fabricated triangular volumetric flip-chip devices have a side dimension of 400 μm. Figure 1 shows a scanning electron microscope image of a typical device and a sketch of its architecture. In contrast to the previous work,⁶ both the n- and p-contacts are formed on the bottom of the structure. The fabricated devices emit at a wavelength of ~415 nm at 85 °C and 220 A/cm².

To characterize device performance, we measure the power conversion efficiency (η_{PCE}) (also called “wall-plug efficiency”) at temperatures of 25 °C and 85 °C (using short electrical pulses to avoid additional heating). η_{PCE} is the ratio of emitted optical power to injected electrical power and is the most important figure of merit for LED efficiency. For

the measurement, the LED is placed in a standard package and encapsulated with a silicone of index $n = 1.41$. These results are therefore representative of real-world devices. Furthermore, 85 °C data are representative of realistic operation and hence guided the optimization process. Figure 2(a) shows the measured η_{PCE} : at 25 °C, it peaks at 84% and is moderately reduced at high current density, with a value of 70% at 100 A/cm². Moreover, this performance level is maintained at 85 °C.

In order to better understand how this high efficiency is obtained, we breakdown η_{PCE} into its basic contributions

$$\eta_{PCE} = \underbrace{PE_V \times C_{ex} \times \eta_{IQE}}_{\eta_{EQE}} \times \eta_{elec}, \quad (1)$$

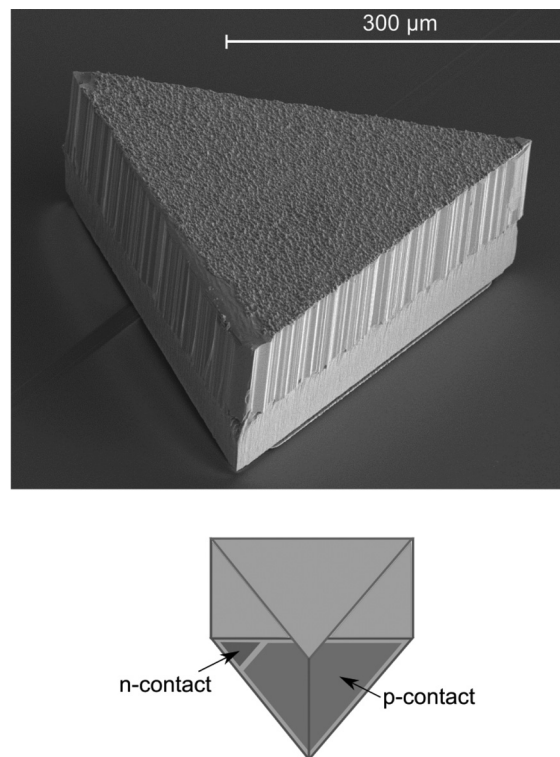


FIG. 1. Scanning electron microscope image of the triangular volumetric flip-chip device (top) and corresponding schematic (bottom).

^{a)}churni@soraa.com

where PE_V is the package efficiency, C_{ex} is the extraction efficiency, η_{IQE} is the internal quantum efficiency, η_{EQE} is the external quantum efficiency, and η_{elec} is the electrical efficiency. With respect to the previous results,⁶ the latter four parameters have been optimized to obtain a high η_{PCE} under typical operating conditions.

PE_V is the ratio of emitted photons by the chip to photons escaping the test package. The package used here was not especially optimized for high extraction as it is only a test vehicle. However, PE_V must still be estimated in order to remove its contribution from η_{PCE} . To this effect, PE_V was modeled using ray tracing software, taking care to include accurate loss values (including their angular dependence) for all materials. We obtained $PE_V = 94\%$.

C_{ex} is the extraction efficiency, which is the ratio of photons escaping the LED to photons radiated by the active region. The issue of light extraction is a well-known problem and various strategies have been explored to address it.⁸ Recently, we showed that C_{ex} was limited in thin-film LED architectures and that volumetric LEDs can improve upon this.^{6,9} Namely, it is possible to combine surface roughness and chip shaping¹⁰ in order to extract all trajectories of light more efficiently. In the present devices, we used a triangular chip shape and added roughness to all exposed surfaces. Advanced modeling shows that this geometry can increase C_{ex} by up to 10% over thin-film device structures.^{6,9} In addition, the reflectivity of the metallic electrical contacts was improved in order to reduce optical loss.

In order to accurately estimate the value of C_{ex} , we performed the dedicated study presented in Ref. 11, where predictions of a light extraction model were compared to experimental performance of a series of devices; this study confirmed the accuracy of the model, which indicates that C_{ex} reaches a value of $\sim 90\%$ in the present device architecture.

η_{IQE} is the ratio of photons emitted from the active region to injected electrons. η_{IQE} is influenced by various factors including defects, active region design, current-density-induced droop (which we will simply call droop in the following), and thermal effects. Defects such as dislocations cause non-radiative recombination, so the use of a low-dislocation density bulk GaN substrate is beneficial. Under high-power operation, radiative recombination must also compete with droop and thermal effects to maintain η_{IQE} . Again, a bulk GaN substrate offers more freedom in designing the active region to achieve this. In general, it is not trivial to separate the values of C_{ex} and η_{IQE} . Here, however, since we have separately determined the value of C_{ex} ,¹¹ we can derive the value of η_{IQE} from the measurement of η_{PCE} , using Eq. (1). The result is shown in Figure 2(b): η_{IQE} peaks at 95% at 25°C and at 92% at 85°C. It also shows low droop with current density, with a value of $\sim 85\%$ at 100 A/cm² and 85°C—a value representative of realistic operating conditions.

We also performed an ABC analysis on η_{IQE} ,¹² including phase-space filling effects.¹³ We note that in the absence of direct lifetime measurements,^{13–16} the parameters A , B , and C are only determined up to an arbitrary scaling factor. The result, shown in Figure 2(b), fits the data well at both temperatures; when going from 25°C to 85°C, the values of A and

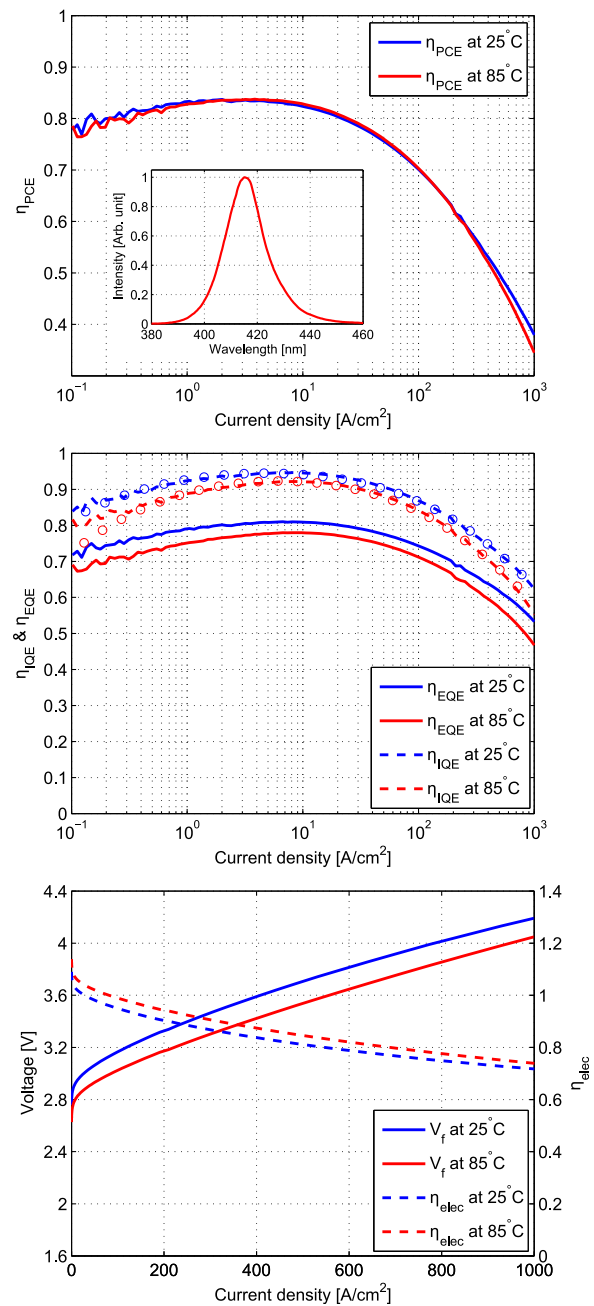


FIG. 2. Device performance. (a) η_{PCE} , with emission spectrum at 85°C and 220 A/cm² in the inset. (b) η_{IQE} and η_{EQE} for the same device. The open symbols are the ABC fits of η_{IQE} . (c) V_f and η_{elec} for the same device.

B had to be slightly increased and decreased, respectively, as can be expected from standard recombination trends in semiconductors. These good fits are consistent with our interpretation of the underlying physics, namely, that Auger scattering with a roughly n^3 dependence is the most plausible mechanism for droop.^{12,13,15,17–21}

Finally, the electrical efficiency η_{elec} is controlled by the forward voltage V_f and is defined here as the ratio of the photon energy to the potential energy of injected electrons: $\eta_{elec} = \hbar\omega/eV_f$. Various factors contribute to V_f : contact resistance, series resistance of the doped epilayers and the dynamic resistance of the LED. Figure 2(c) shows V_f and η_{elec} as a function of the current density. The associated series resistance is $\sim 1 \times 10^{-3} \Omega \text{ cm}^2$. This value is about an

order of magnitude lower than state-of-the-art thin-film devices,²² which is instrumental for operation at high current density. The low R_s value was obtained by optimizing the contact resistances, while maintaining a high contact reflectivity. Through transfer-length measurements, we estimate that the p-contact and n-contact specific resistances are $\sim 2 \times 10^{-4} \Omega \text{ cm}^2$ and $\sim 3 \times 10^{-5} \Omega \text{ cm}^2$, respectively. It can be noticed that V_f decreases appreciably between 25 °C and 85 °C; this is because the structure was designed for optimal injection at 85 °C. In fact, this effect compensates the drop in η_{IQE} and results in a nearly constant η_{PCE} .

A potential concern for flip-chip devices is current crowding which is often associated with lateral injection, because current has a tendency to crowd at the edge of the contacts.²³ Current crowding is problematic for various reasons including reliability concerns, higher local current density which reduces η_{IQE} , localized heating, etc. Here again, the use of bulk GaN substrates is particularly advantageous as it provides a thick, highly conductive layer which improves current spreading.

To illustrate this, we performed simulations of electrical injection in various device structures using finite element modeling. To check the accuracy of the model, we verified that the calculated current-voltage characteristic matched that of our experimental devices. Figure 3(a) compares the calculated vertical current density J_z in two devices: a LED with a 150 μm conductive bulk GaN substrate (similar to our actual devices) and the same structure with a 10 μm substrate

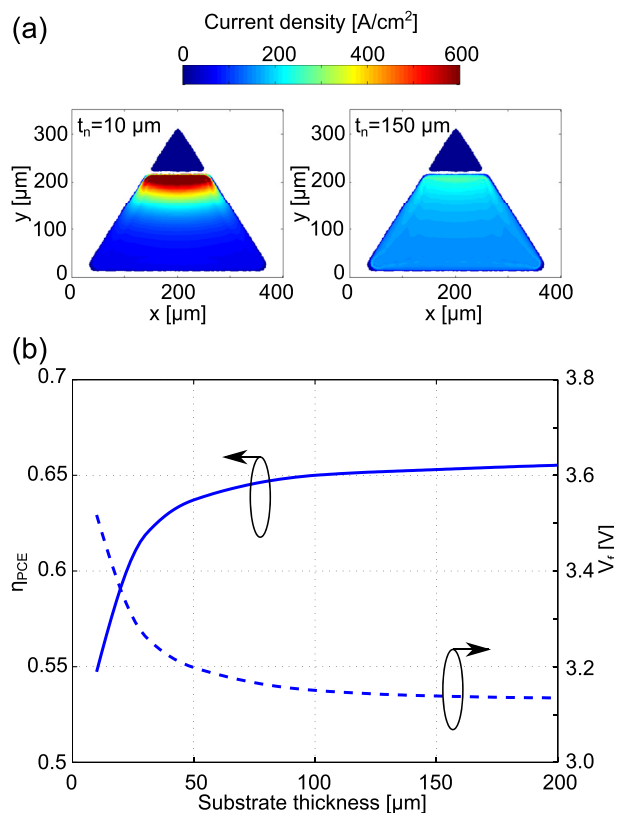


FIG. 3. Finite element modeling of current spreading. (a) Vertical component of the current density J_z across the active region for a device with 10 μm (left) and 150 μm (right) of highly conductive GaN. (b) Effect of the GaN substrate thickness on V_f and η_{PCE} . For both (a) and (b), the average current density injected in the device is 160 A/cm^2 at a temperature of 85 °C.

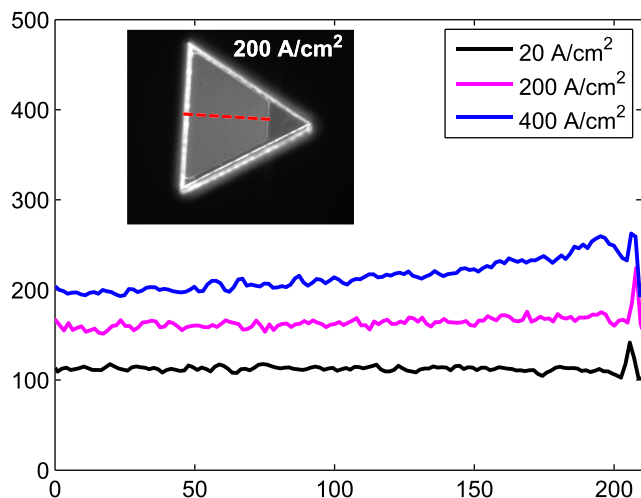


FIG. 4. Plot of light intensity obtained from microscope pictures at three current densities. The amplitude of each curve was rescaled by an arbitrary factor for clarity. The cross-section used is shown in dashed lines in the inset (picture at 200 A/cm^2).

(both at a current density of 160 A/cm^2 and a temperature of 85 °C): the thinner substrate induces significant current crowding. As shown in Figure 3(b), it also causes a higher V_f , leading to a reduction of η_{PCE} by more than 10%.

The absence of current crowding in our devices is confirmed experimentally: in Figure 4, the light intensity profile of a lit LED is shown at three current densities (the top surface of the device was polished in order to image the light emission). Even at the highest drive condition, current crowding is very moderate.

As a final comment on electrical performance, we note that η_{elec} reaches values above unity for current densities below 75 A/cm^2 , which indicates that the emitted photons have a higher energy than the injected electrons. This interesting effect is commonly observed at low current density in high-performance LEDs, but is seldom discussed. It is caused by the tail of the statistical distribution of injected carriers which enables recombination at energies above eV_f (in other words, carriers absorb energy from phonon scattering before they recombine so that overall energy conservation is satisfied).²⁴⁻²⁶ This effect is sometimes thought to only be prevalent under low injection conditions; therefore, it is noteworthy that in the present devices it is still significant at fairly high current density.

Each of the figures of merit reported here is equivalent or superior to previously reported results for III-nitride LEDs and illustrates the unique advantages of bulk GaN technology. Indeed, other approaches lead to tradeoffs between figures of merit: for instance, the improvement of electrical efficiency is often detrimental to extraction efficiency (as larger or more lossy contacts must be used); this makes it challenging to operate at high power density in such devices, so that most real-world LEDs are restricted to moderate drive conditions. With bulk-GaN technology, all characteristics can be optimized simultaneously, thus enabling truly high power density operation.

In conclusion, we presented results from violet III-nitride LEDs grown on bulk GaN substrates which employ a triangular volumetric flip-chip architecture. We demonstrated that the

use of bulk GaN substrates systematically enables improved performance over standard LED technology: superior internal quantum efficiency, extraction efficiency and electrical efficiency. All these properties combine to allow efficient high power operation, as required by the most challenging applications in solid-state lighting. These devices exhibit the highest power conversion efficiency reported to date at high current density and high temperature.

- ¹S. Nakamura, T. Mukai, and M. Senoh, *Appl. Phys. Lett.* **64**, 1687 (1994).
- ²J. J. Wierer, J. Y. Tsao, and D. S. Sizov, *Laser Photonics Rev.* **7**, 963 (2013).
- ³H. Geng, H. Sunakawa, N. Sumi, K. Yamamoto, A. A. Yamaguchi, and A. Usui, *J. Cryst. Growth* **350**, 44 (2012).
- ⁴T. Yoshida, Y. Oshima, T. Eri, K. Ikeda, S. Yamamoto, K. Watanabe, M. Shibata, and T. Mishima, *J. Cryst. Growth* **310**, 5 (2008).
- ⁵P. Hageman, V. Kirilyuk, W. Corbeek, J. Weyher, B. Lucznik, M. Bockowski, S. Porowski, and S. Mueller, *J. Cryst. Growth* **255**, 241 (2003).
- ⁶M. J. Cich, R. I. Aldaz, A. Chakraborty, A. David, M. J. Grundmann, A. Tyagi, M. Zhang, F. M. Steranka, and M. R. Krames, *Appl. Phys. Lett.* **101**, 223509 (2012).
- ⁷J. J. Wierer, D. A. Steigerwald, M. R. Krames, J. J. O'Shea, M. J. Ludowise, G. Christenson, Y.-C. Shen, C. Lowery, P. S. Martin, S. Subramanya, W. Gtz, N. F. Gardner, R. S. Kern, and S. A. Stockman, *Appl. Phys. Lett.* **78**, 3379 (2001).
- ⁸C. Lalau Keraly, L. Kuritzky, M. Cochet, and C. Weisbuch, in *III-Nitride Based Light Emitting Diodes and Applications*, Topics in Applied Physics, Vol. 126, edited by T.-Y. Seong, J. Han, H. Amano, and H. Morkoc (Springer, the Netherlands, 2013), pp. 231–269.
- ⁹A. David, *J. Disp. Technol.* **9**, 301 (2013).
- ¹⁰M. R. Krames, M. Ochiai-Holcomb, G. E. Hfler, C. Carter-Coman, E. I. Chen, I.-H. Tan, P. Grillot, N. F. Gardner, H. C. Chui, J.-W. Huang, S. A. Stockman, F. A. Kish, M. G. Craford, T. S. Tan, C. P. Kocot, M. Hueschen, J. Posselt, B. Loh, G. Sasser, and D. Collins, *Appl. Phys. Lett.* **75**, 2365 (1999).
- ¹¹A. David, C. A. Hurni, R. I. Aldaz, M. J. Cich, B. Ellis, K. Huang, F. M. Steranka, and M. R. Krames, *Appl. Phys. Lett.* **105**, 231111 (2014).
- ¹²Y. Shen, G. Mueller, S. Watanabe, N. Gardner, A. Munkholm, and M. Krames, *Appl. Phys. Lett.* **91**, 141101 (2007).
- ¹³A. David and M. J. Grundmann, *Appl. Phys. Lett.* **96**, 103504 (2010).
- ¹⁴P. G. Eliseev, M. Osinski, H. Li, and I. V. Akimova, *Appl. Phys. Lett.* **75**, 3838 (1999).
- ¹⁵A. David and M. J. Grundmann, *Appl. Phys. Lett.* **97**, 033501 (2010).
- ¹⁶W. G. Scheibenzuber, U. T. Schwarz, L. Sulmoni, J. Dorsaz, J.-F. Carlin, and N. Grandjean, *J. Appl. Phys.* **109**, 093106 (2011).
- ¹⁷N. F. Gardner, G. O. Miller, Y. C. Shen, G. Chen, S. Watanabe, W. Goetz, and M. R. Krames, *Appl. Phys. Lett.* **91**, 243506 (2007).
- ¹⁸A. David and N. F. Gardner, *Appl. Phys. Lett.* **97**, 193508 (2010).
- ¹⁹E. Kioupakis, P. Rinke, K. T. Delaney, and C. G. Van de Walle, *Appl. Phys. Lett.* **98**, 161107 (2011).
- ²⁰J. Iveland, L. Martinelli, J. Peretti, J. S. Speck, and C. Weisbuch, *Phys. Rev. Lett.* **110**, 177406 (2013).
- ²¹M. Binder, A. Nirschl, R. Zeisel, T. Hager, H.-J. Lugauer, M. Sabathil, D. Bougeard, J. Wagner, and B. Galler, *Appl. Phys. Lett.* **103**, 071108 (2013).
- ²²Y. Narukawa, M. Ichikawa, D. Sanga, M. Sano, and T. Mukai, *J. Phys. D: Appl. Phys.* **43**, 354002 (2010).
- ²³X. Guo and E. F. Schubert, *Appl. Phys. Lett.* **78**, 3337 (2001).
- ²⁴J. Tauc, *Czech. Fiz. Z.* **7**, 275 (1957).
- ²⁵R. Keyes and T. Quist, *Proc. IRE* **50**, 1822 (1962).
- ²⁶P. Santhanam, D. J. Gray, and R. J. Ram, *Phys. Rev. Lett.* **108**, 097403 (2012).